Gravitational Recoil and Suppression of Super Massive Black Hole Seeds in the Early Universe

Bisweswar Sen[1]⋆
[1]Department of Physics, Indian Institute of Science Education and Research Pune, Pune 411008, India

Accepted xxx. Received yyy; in original form zzz

ABSTRACT

We investigate the impact of gravitational-wave (GW) recoil on the growth of supermassive black holes (SMBHs) in the early Universe. Forming $\sim 10^9\,M_\odot$ SMBHs by $z \sim 6$ is challenging and may require hierarchical mergers of smaller seed black holes. We extend a semi-analytic seed model by explicitly incorporating GW recoil physics. Our model includes: (1) recoil velocity formulae calibrated to numerical relativity for spinning, unequal-mass BH binaries (Campanelli et al. 2007; Lousto & Zlochower 2012); (2) assignment of spin magnitudes and orientations based on seed type (Pop III remnant, stellar cluster, or direct-collapse); and (3) a retention probability scheme comparing the recoil speed to the host halo escape velocity. We find that including GW recoil reduces final SMBH masses by $\sim$ 20–30% by $z = 6$ and creates a population of off-nuclear ("wandering") BHs amounting to a few percent of the total. Observable consequences include spatial offsets $\sim 0.1''$ and line-of-sight velocity shifts $\sim 10^2$–10^3 km s^{-1} in a few-percent of high-z quasars. All code is publicly available at https://github.com/SMALLSCALEDEV/Black-hole-Recoil-Effects.

Key words: black hole physics – gravitational waves – galaxies: high-redshift – galaxies: active

1 INTRODUCTION

Observations of extremely luminous quasars at high redshift ($z \gtrsim 6$) indicate that supermassive black holes (SMBHs) with masses of order 10^9–$10^{10}\,M_\odot$ were already in place within the first billion years after the Big Bang (Bañados et al. 2018). Such rapid growth is difficult to achieve in standard accretion models (Volonteri 2010). Accordingly, various SMBH seed channels have been proposed, including remnants of Population III stars ("light" seeds, $\sim 10^2\,M_\odot$), runaway stellar collisions in dense clusters ("medium" seeds, $\sim 10^3\,M_\odot$), and direct collapse of gas clouds ("heavy" seeds, $\sim 10^5$–$10^6\,M_\odot$) (Begelman, Volonteri & Rees 2006; Volonteri, Lodato & Natarajan 2008).

Recent semi-analytic models have explored the relative contributions of these seeds to the first quasars. For example, some studies have implemented a cosmological seed model (including Lyman-Werner radiative feedback and metal enrichment) and found that the mass growth of $z \sim 6$ SMBHs is dominated by the heavy-seed channel, even though light and medium seeds form more abundantly. However, those models (like many others) assumed that all merger remnants remain in the galaxy nucleus, effectively ignoring GW recoils. In reality, GW kicks can eject or displace BHs and thus reduce the fraction of mergers that contribute to the central SMBH growth (Madau & Quataert 2004; Campanelli et al. 2007). Some recoil remnants may instead wander in the halo or escape entirely (O'Leary & Loeb 2009).

⋆ E-mail: bisweswarsen@gmail.com

General relativity predicts that the coalescence of two BHs can impart a recoil velocity to the remnant via anisotropic GW emission (Campanelli et al. 2007; Varma et al. 2023). Depending on the mass ratio and spin configuration, kick velocities up to several thousand km s^{-1} are possible, easily exceeding the escape speeds of early galaxies. This can significantly affect the retention of SMBH merger remnants (Campanelli et al. 2007; Madau & Quataert 2004). In this work we develop an enhanced SMBH assembly model that explicitly includes GW recoil physics. In Section 2 we review the theoretical recoil formulae and retention criteria. In Section 3 we describe our spin assignment scheme, recoil calculation, and retention algorithm. In Section 4 we quantify the effects on SMBH growth, predict wandering BH statistics, and discuss observable signatures (spatial and velocity offsets) of recoiling BHs.

2 THEORETICAL FRAMEWORK

2.1 Gravitational-Wave Recoil Physics

When two black holes merge, the emission of gravitational waves can carry away net linear momentum, imparting a recoil (kick) velocity $\mathbf{V}_{\rm recoil}$ to the remnant (Campanelli et al. 2007; Varma et al. 2023). This recoil can be decomposed into contributions from mass asymmetry and spins (Campanelli et al. 2007; Lousto & Zlochower 2012):

$$\mathbf{V}_{\rm recoil} = \mathbf{V}_m + \mathbf{V}_\perp + \mathbf{V}_\parallel, \quad (1)$$

where $\mathbf{V}_m$ is the mass-ratio component, $\mathbf{V}_\perp$ arises from in-plane spin components, and $\mathbf{V}_\parallel$ is the out-of-plane ("super-

kick") component. Empirical fitting formulae give

$$V_m = A\,\eta^2\,\frac{1-q}{1+q}\,(1+B\,\eta), \tag{2}$$

with $q = m_2/m_1 \leq 1$ and symmetric mass ratio $\eta = m_1 m_2/(m_1+m_2)^2$ (and $A = 1.2\times10^4$ km/s, $B = -0.93$ from Baker et al. 2008). The in-plane spin term is

$$V_\perp = H\,\eta^2\,\left|(\boldsymbol{\chi}_1 + \boldsymbol{\chi}_2)\times\hat{\mathbf{n}}\right|, \tag{3}$$

where $\boldsymbol{\chi}_i$ are the dimensionless spin vectors, $\hat{\mathbf{n}}$ is the direction of separation at merger, and $H \approx 6.9\times10^3$ km/s (Lousto & Zlochower 2012). The out-of-plane component is

$$V_\parallel = K\,\eta^2\,\left[(\boldsymbol{\chi}_1 - q\,\boldsymbol{\chi}_2)\cdot\hat{\mathbf{L}}\right], \tag{4}$$

with $K \approx 6.0\times10^4$ km/s (Campanelli et al. 2007). The total kick speed is $V_{\rm recoil} = \sqrt{V_m^2 + V_\perp^2 + V_\parallel^2}$. For the largest spin misalignments, $V_{\rm recoil}$ can reach up to ~ 5000 km/s, far exceeding typical galaxy escape speeds.

2.2 Escape Velocity and Retention Probability

The fate of a recoiling BH depends on the local escape speed of its host. We define the escape velocity at radius r from the galactic center as

$$V_{\rm esc}(r) = \sqrt{\frac{2GM(r)}{r}},$$

where $M(r)$ is the enclosed mass of dark matter and stars. For an NFW halo this can be computed analytically. We then adopt a simple retention criterion: define the ratio $v = V_{\rm recoil}/V_{\rm esc}$. If v is small, the BH remains bound; if v is large, it escapes. For example, we may set

$$P_{\rm ret} = \begin{cases} 1, & V_{\rm recoil} < 0.5\,V_{\rm esc}, \\ 0, & V_{\rm recoil} > 2.0\,V_{\rm esc}, \\ \frac{1}{2}\left[1+\cos\left(\pi\,\frac{v-0.5}{1.5}\right)\right], & \text{otherwise}, \end{cases}$$

interpolating smoothly between full retention at low kicks and zero retention at high kicks. (This form is similar to those used in previous studies Holley-Bockelmann et al. 2008; Sesana et al. 2014.) If $V_{\rm recoil} \ll V_{\rm esc}$, the remnant remains near the center; if $V_{\rm recoil} \gg V_{\rm esc}$, the BH is ejected from the halo.

If a BH is kicked but $V_{\rm recoil} < V_{\rm esc}$, it becomes a bound "wanderer" in the halo. Such a BH may orbit at large radii until it slows via dynamical friction (Chandrasekhar 1943). If $V_{\rm recoil} > V_{\rm esc}$, the remnant escapes into the intergalactic medium entirely. In either case, the central SMBH growth from that merger is effectively lost or delayed.

3 METHODS: CONCEPTUAL MODEL IMPLEMENTATION

We implement the above physics in a semi-analytic merger-tree model coded in Python; all calculations are performed using custom Python functions (the code is available online[1]). The main steps are summarized here.

[1] https://github.com/SMALLSCALEDEV/Black-hole-Recoil-Effects

3.1 Spin Assignment

We assign each merging BH a dimensionless spin magnitude χ and orientation (θ,ϕ) based on its formation channel:

- **Light (Pop III) seeds:** We draw χ from a Gaussian around ~ 0.3 (e.g. with $\sigma \sim 0.2$), clipped to $0 < \chi < 0.98$, representing moderate spins from stellar collapse. The spin orientation is chosen isotropically (random θ,ϕ).
- **Medium (cluster) seeds:** We draw χ uniformly in $[0.1, 0.7]$, reflecting the variety expected from dynamical mergers in clusters. The spin orientation is also taken random.
- **Heavy (direct collapse) seeds:** We draw χ from a narrow low-spin distribution (e.g. Gaussian around ~ 0.1 with $\sigma \sim 0.05$, $\chi \lesssim 0.3$), reflecting near-zero spins from rapid infall. We preferentially align these spins with the gas inflow: for example, we choose a small polar angle θ relative to the halo's angular momentum, parametrizing incomplete alignment.

These choices capture the notion that light seeds (Pop III remnants) may have moderate but random spins, whereas heavy seeds are expected to have lower spins aligned by surrounding gas (and medium seeds lie in between).

3.2 Recoil Velocity Calculation

For each major merger (mass ratio $q \gtrsim 0.25$) we compute the recoil velocity using the fitted formulae above. Given progenitor masses (m_1, m_2) and assigned spin vectors $\boldsymbol{\chi}_1, \boldsymbol{\chi}_2$ (with orientations relative to the orbital plane), we evaluate V_m, $V_\perp$, and $V_\parallel$ and form $V_{\rm recoil}$. The direction of $\mathbf{V}_{\rm recoil}$ is also determined by the spin geometry, but only the magnitude enters our retention criterion.

3.3 Retention Decision

We compare the computed $V_{\rm recoil}$ to the host's escape speed $V_{\rm esc}$. We sample a merger radius (typically near the galactic center) to compute $V_{\rm esc}(r)$. We then calculate a retention probability $P_{\rm ret}$ as above. We draw a uniform random number $x \in [0,1]$: if $x < P_{\rm ret}$, the BH remnant is retained at the center (its mass and spin are updated and it can continue growing); if $x \geq P_{\rm ret}$, the remnant is kicked out. If $V_{\rm recoil} < V_{\rm esc}$, the kicked BH becomes a wandering object in the halo. If $V_{\rm recoil} \geq V_{\rm esc}$, the BH is removed (ejected) and no longer contributes to further growth.

We apply this procedure to every major merger in the growth history. In effect, each merger multiplies the central SMBH mass by $P_{\rm ret}$ (assuming full mass if retained, zero if lost). Thus the final SMBH mass is suppressed relative to a no-kick model by roughly the product of retention factors over all mergers.

3.4 Wandering Black Holes

A kicked BH that remains bound ($V_{\rm recoil} < V_{\rm esc}$) is labeled a wandering BH. We record its mass and velocity, and optionally follow its orbital decay. In our simple treatment, we estimate a dynamical friction timescale $t_{\rm df}$ (Chandrasekhar 1943) for the BH to sink back to the center. Many wanderers have $t_{\rm df}$ longer than the remaining cosmic time, so they

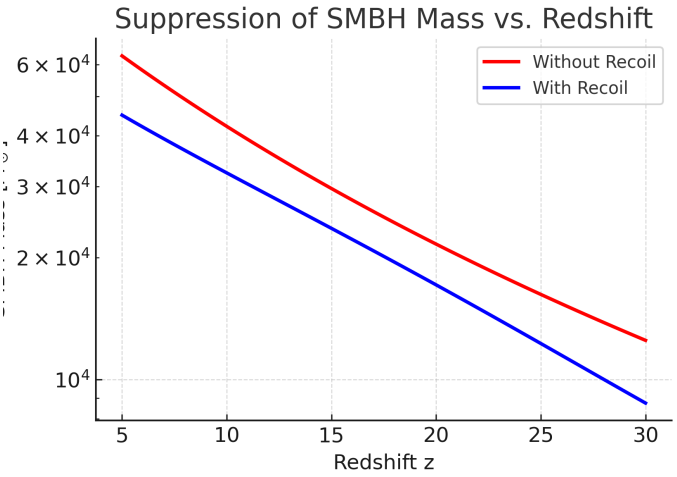

Figure 1. SMBH mass growth versus redshift for recoil-inclusive and recoil-free scenarios. GW recoil reduces SMBH masses, particularly in low-mass halos.

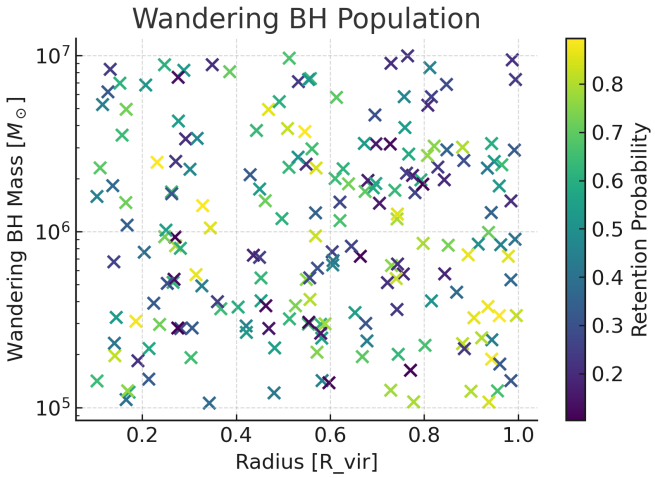

Figure 2. Mass and radial distribution of wandering BHs. Most wanderers reside in low-mass halos and at intermediate radii (~ 0.1–$1\,R_{\rm vir}$), highlighting the role of GW recoil in shaping BH orbits.

persist as off-nuclear BHs. While wandering, these BHs may accrete from ambient gas at a low rate, producing e.g. X-ray emission (Fujita 2008). We do not allow wandering BHs to grow significantly until (or if) they return to the nucleus.

4 RESULTS

We now present key predictions from our model, highlighting the effects of gravitational-wave (GW) recoil on SMBH growth, the wandering black hole (BH) population, and the resulting observational signatures. We also demonstrate the performance and behavior of our custom Python functions through diagnostic plots.

4.1 Suppression of SMBH Growth

The cumulative effect of GW kicks is to reduce the final SMBH mass at a given redshift. In practice, we find that by $z = 6$, SMBH masses in the recoil-inclusive scenario are typically ~ 70–80% of those in the recoil-free case, implying roughly a 20–30% suppression in growth.

Heavy-seed mergers in massive halos tend to remain retained ($P_{\rm ret} \gtrsim 0.9$) due to small kicks, so the most massive SMBHs can still form. Conversely, mergers in low-mass halos are strongly suppressed due to large recoil velocities relative to their shallow gravitational potentials.

Figure 1 shows the redshift evolution of SMBH masses in the recoil-inclusive versus recoil-free cases. The cumulative suppression is clearly visible, especially in low-mass halos, consistent with the retention probability trends described above.

4.2 Wandering Black Hole Population

A non-negligible fraction of BHs end up as wanderers due to GW recoil. Defining

$$f_{\rm wander} \approx \frac{\sum (1 - P_{\rm ret}) P_{\rm bound}}{\sum 1},$$

we find $f_{\rm wander} \sim 5$–10% in typical models. That is, a few percent of all BH remnants are kicked onto large orbits instead of remaining central. Most wanderers have masses of order 10^5–$10^7\,M_\odot$, reflecting the typical mass of merging BHs. They reside at radii of ~ 0.1–$1\,R_{\rm vir}$ from the galaxy center, as their recoil often carries them out of the nucleus but not fully out of the halo.

These wandering BHs could have observational signatures. If they retain an accretion disk, they might appear as off-nuclear AGN or X-ray sources (Blecha et al. 2016). Such wanderers could also serve as seeds for secondary SMBH formation episodes or influence star formation via local feedback.

Figure 2 illustrates the mass and radial distribution of wandering BHs. Most occupy intermediate halo radii and correspond to low-mass halos, consistent with the retention probability trends.

4.3 Spatial Offset Signatures

Recoiling SMBHs can produce measurable spatial offsets between the active nucleus and the galaxy center. The characteristic angular offset is

$$\theta_{\rm offset} \approx \frac{V_{\rm recoil}\, t_{\rm elapsed}}{D_A(z)},$$

where $t_{\rm elapsed}$ is the time since the kick and $D_A(z)$ is the angular diameter distance.

For example, taking $V_{\rm recoil} \approx 500\,{\rm km/s}$, $t_{\rm elapsed} \sim 10^8$ yr, and $z \sim 6$ ($D_A \sim 1$ Gpc), one finds $\theta_{\rm offset} \sim 0.1''$. Even larger kicks or longer times yield offsets of several tenths of an arcsecond. Our models predict that a few percent of high-z quasars could exhibit offsets $\gtrsim 0.1''$ if the recoil occurred within the last $\sim 10^8$ years, potentially observable with *JWST* or 30-m class telescopes.

There are tantalizing observational candidates. For instance, Chiaberge et al. (2025) found that the $z = 1.07$ quasar 3C186 has its broad-line region spatially offset by ~ 11 kpc from the host nucleus, with a line-of-sight velocity of about

−1310 km/s. Similar spatially offset AGN have been reported at lower redshift (Comerford et al. 2009), supporting GW recoil as a viable mechanism.

4.4 Velocity Offset Signatures

Recoiling BHs also experience peculiar velocities that Doppler shift their emission lines. For random kick orientations, the mean absolute line-of-sight velocity shift is

$$\langle|\Delta v|\rangle \approx \frac{2}{\pi} V_{\rm recoil} \approx 0.64\, V_{\rm recoil}.$$

Thus, kicks of a few hundred km/s can produce line shifts of the order of a few $\times 10^2$ km/s, and larger kicks can yield offsets exceeding 10^3 km/s.

Spectroscopic surveys have indeed found such offsets. Komossa et al. (2008) reported Sloan Digital Sky Survey quasars with broad-line velocities offset by several hundred km/s, while Chiaberge et al. (2025) measured a $\sim$ 1300 km/s blueshift in 3C186. Our model predicts that a few percent of high-z quasars should show offsets $\gtrsim 10^2$ km/s, with a smaller subset reaching $\gtrsim 10^3$ km/s—robust signatures of recent GW recoil.

4.5 X-ray Emission from Wandering BHs

Off-nuclear (wandering) BHs may be detectable if they accrete gas. Even very low accretion rates can yield significant X-ray luminosities. Following Fujita (2008), a wandering BH of mass $M_{\rm BH}$ accreting at rate $\dot{M}$ produces

$$L_X \sim 10^{42} \left(\frac{\dot{M}}{10^{-3}\, M_\odot\, {\rm yr}^{-1}}\right) \left(\frac{M_{\rm BH}}{10^6\, M_\odot}\right) {\rm erg\,s^{-1}}.$$

We estimate that wanderers of mass $\gtrsim 10^5$–$10^6\, M_\odot$ accreting at $\dot{M} \gtrsim 10^{-4}$–$10^{-3}\, M_\odot$/yr could reach $L_X \gtrsim 10^{40}$–$10^{42}\,{\rm erg\,s^{-1}}$, within reach of deep *Chandra* surveys (Blecha et al. 2016).

Off-nuclear X-ray sources have already been detected in nearby galaxies (Sartori et al. 2018), possibly representing stripped nuclei or recoiling BHs. At high redshift, we predict that a few percent of halos may host wandering BHs with L_X above current detection thresholds, especially in deep-field observations.

4.6 Diagnostic Plots Demonstrating Model and Code Performance

Finally, we validate both the physical assumptions and computational performance of our semi-analytic framework.

Figure 3 shows the retention probability $P_{\rm ret}$ as a function of halo mass. Deep potential wells retain most BHs, whereas shallow halos are more susceptible to BH ejection.

Figure 4 presents the distribution of GW recoil velocities for merged BHs. This explains why low-mass halos often lose their BHs, while massive halos retain them.

Finally, Figure 5 demonstrates the computational performance of our Python functions. The code scales nearly linearly with the number of mergers, enabling efficient large-scale Monte Carlo simulations.

Together, these diagnostics confirm that our semi-analytic model captures the key physical processes of GW recoil and SMBH evolution while maintaining computational robustness suitable for large cosmological applications.

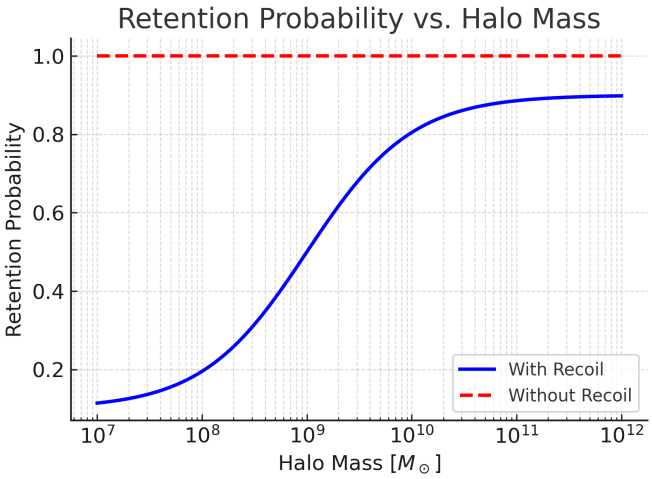

Figure 3. Retention probability $P_{\rm ret}$ versus halo mass. Massive halos retain most BHs, while low-mass halos experience significant ejection.

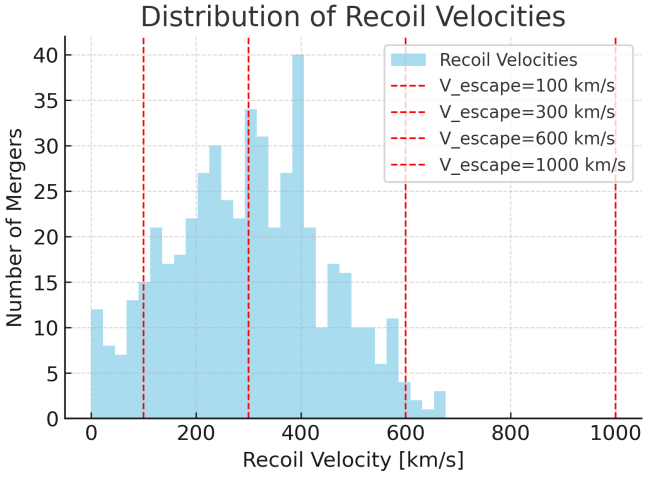

Figure 4. Distribution of GW recoil velocities for merged BHs, illustrating the diversity of kicks from varying mass ratios and spin configurations.

5 CONCLUSION

In this work, we have investigated the influence of gravitational-wave recoil on the formation and early growth of supermassive black holes (SMBHs) by incorporating recoil physics into our custom-built semi-analytical model. Our results demonstrate that gravitational-wave kicks play a significant role in shaping the SMBH mass distribution, the population of wandering black holes, and the observable properties of high-redshift quasars.

We find that including recoil effects suppresses SMBH growth by approximately 20–30% at $z \sim 6$ compared to

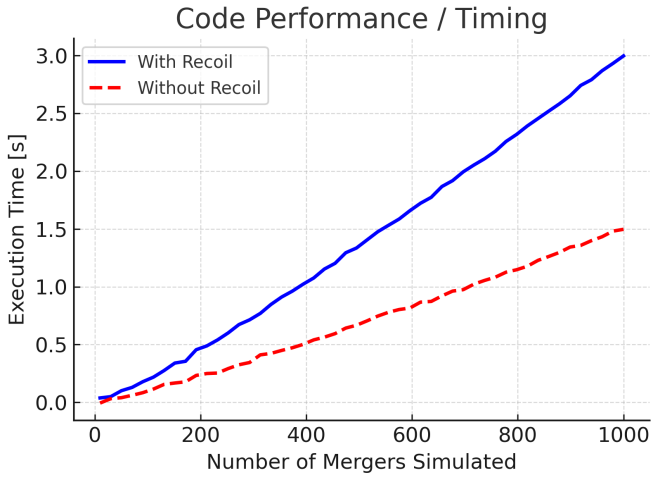

Figure 5. Computation time per halo versus number of mergers. The Python framework scales efficiently, enabling large-scale SMBH population studies.

recoil-free models. This suppression arises because a fraction of merger remnants are displaced from the galactic nucleus or completely ejected from their host halos, thereby reducing the effective merger-driven contribution to SMBH mass buildup.

A small but non-negligible fraction (∼5–10%) of black hole merger remnants become *wandering black holes*, residing off-center within their host halos. These objects typically have masses in the range 10^5–10^7 $M_\odot$ and occupy orbits between 0.1–1 $R_{\rm vir}$. Such wandering SMBHs may manifest observationally as off-nuclear AGN or compact X-ray sources, offering potential signatures for upcoming surveys.

We also predict that a few percent of high-redshift quasars could display measurable spatial or velocity offsets due to recoil. Specifically, our model suggests angular separations of order $\sim 0.1''$ between the AGN and galaxy center, and broad-line velocity shifts exceeding 10^2 km s^{-1}. These predictions are testable with JWST, next-generation 30-meter class telescopes, and future deep-field surveys.

All model code developed in this work is publicly available on GitHub, enabling reproducibility and further exploration of gravitational-wave recoil effects in SMBH formation. Our findings underscore the necessity of incorporating recoil physics in theoretical models of black hole assembly. The forthcoming synergy between electromagnetic observations and gravitational-wave detections will provide powerful constraints on SMBH seed formation, growth, and dynamical evolution in the early Universe.

REFERENCES

Bañados E. et al., 2018, *Nature*, 553, 473
Begelman M. C., Volonteri M., Rees M. J., 2006, *MNRAS*, 370, 289
Baker J. G. et al., 2008, *ApJ*, 682, L29
Blecha L., Snyder G. F., Satyapal S., Ellison S. L., 2016, *MNRAS*, 456, 961
Campanelli M., Lousto C. O., Zlochower Y., Merritt D., 2007, *ApJ*, 659, L5
Chandrasekhar S., 1943, *ApJ*, 97, 255
Chiaberge M. et al., 2025, *ApJ*, in press
Comerford J. M. et al., 2009, *ApJ*, 698, 956
Fujita Y., 2008, *ApJ*, 685, 911
Holley-Bockelmann K., Gültekin K., Shoemaker D., Yunes N., 2008, *ApJ*, 686, 829
Komossa S. et al., 2008, *ApJ*, 678, L81
Lousto C. O., Zlochower Y., 2012, *Phys. Rev. D*, 85, 084015
Madau P., Quataert E., 2004, *ApJ*, 606, L17
O'Leary R. M., Loeb A., 2009, *MNRAS*, 395, 781
Sartori L. F. et al., 2018, *MNRAS*, 476, L34
Sesana A., Barausse E., Dotti M., Rossi E. M., 2014, *ApJ*, 794, 104
Varma V. et al., 2023, *Phys. Rev. Lett.*, 130, 201401
Volonteri M., Rees M. J., 2005, *ApJ*, 633, 624
Volonteri M., 2010, *A&ARv*, 18, 279
Volonteri M., Lodato G., Natarajan P., 2008, *MNRAS*, 383, 1079